Geometric and Topological Approaches to Shape Variation in *Ginkgo* Leaves

Haibin Hang[1*], Martin Bauer[2*], Washington Mio[2], Luke Mander[3]

[1]Department of Mathematical Sciences, University of Delaware, Newark, DE 19716, USA; [2]Department of Mathematics, Florida State University, Tallahassee, FL 32306, USA; [3]School of Environment, Earth and Ecosystem Sciences, The Open University, Milton Keynes, MK7 6AA, UK

*Denotes equal contribution to this work

Author for correspondence:
Luke Mander
Email: luke.mander@gmail.com

Abstract

Leaf shape is a key plant trait that varies enormously. The diversity of leaf shape, and the range of applications for data on this trait, requires frequent methodological developments so that researchers have an up-to-date toolkit with which to quantify leaf shape. We generated a dataset of 468 leaves produced by *Ginkgo biloba*, and 24 fossil leaves produced by evolutionary relatives of extant *Ginkgo*. We quantified the shape of each leaf by developing a geometric method based on elastic curves and a topological method based on persistent homology. Our geometric method indicates that shape variation in our modern sample is dominated by leaf size, furrow depth, and the angle of the two lobes at the base of the leaf that is also related to leaf width. Our topological method indicates that shape variation in our modern sample is dominated by leaf size and furrow depth. We have applied both methods to modern and fossil material: the methods are complementary, identifying similar primary patterns of variation, but also revealing some different aspects of morphological variation. Our topological approach distinguishes long-shoot leaves from short-shoot leaves and both methods indicate that leaf shape influences or is at least related to leaf area.

Key words: Biological shape, plant traits, morphometric methods, elastic curves, persistent homology.

Introduction

Leaf shape is a fascinatingly diverse plant trait. It can vary between taxa, between individuals in different populations of the same species, and for some species there are striking variations in leaf shape within a single plant, a phenomenon known as heterophylly. Additionally, different regions of a leaf expand at different rates during development, and this leads to allometric changes in shape as a leaf grows. Leaves are primary sites of photosynthesis and play a central role in the growth and survival of a plant, and work has shown that variation in leaf shape may be related to thermoregulation, the constraints of hydraulics and mechanics, patterns of leaf expansion, as well as the avoidance of herbivory and the optimal interception of light (Nicotra *et al.*, 2011). Leaf shape is therefore a trait for which there are many functional trade-offs, and from an ecological perspective may be viewed "not as a single major axis, but rather as an option that fine tunes the leaf to its conditions over both short and evolutionary time spans" (Nicotra *et al.*, 2011, p. 547).

The taxonomic and ecological significance of leaf shape has led to the development of numerous methods to characterize this trait. Certain methods rely on largely qualitative observation. For example, aspects of leaf shape can be described using specialist terminology (Leaf Architecture Working Group 1999), which allows leaves to be placed into categories based on their gross morphology, and this approach has proved useful in studies of plant architecture (e.g. Leigh, 1999; Barthelemy & Caraglio, 2007) and studies of fossil leaves that may not be preserved in their entirety (e.g. Johnson, 1992). Other methods for characterising leaf shape are based on morphometric measurements of certain features on a leaf, which can either be made manually by human researchers or computationally using image analysis software. For example, Leigh *et al.* (2011) described leaf shape using measurements of leaf area and leaf dissection (leaf perimeter/area) in the context of plant hydraulics, and Royer *et al.* (2005) used the same measure of leaf dissection to investigate the relationship between mean annual temperature and leaf shape. Measurements of such morphological features are often used to generate indices of leaf shape, such as compactness (perimeter^2/area) and shape factor (4π x leaf area/perimeter^2), which are used to summarize aspects of leaf shape and show how it relates to the environment

or has changed through time (Royer *et al.*, 2008, 2009; Peppe *et al.*, 2011; Bacon *et al.*, 2013). Morphometric techniques that use landmarks (a constellation of discrete anatomical loci, each described by 2- or 3-dimensional Cartesian coordinates to quantify morphology (Thompson 1942; Bookstein 1996; Webster & Sheets, 2010)) have been employed to capture variation in leaf shape (Weight *et al.*, 2008) and have highlighted differing developmental and evolutionary contributions to leaf shape (Chitwood *et al.*, 2016), while elliptic Fourier analysis has been used to quantify leaf outlines (McLellan 1993; Chitwood & Otoni 2017). Persistent homology—a topological data analysis method—has also been applied to the problem of quantifying leaf shape (Li *et al.*, 2018a,b), and represents a morphometric framework to measure plant form that allows comparison of the morphology of different plant organs such as leaves, roots and stems (Bucksch *et al.*, 2017; Li *et al.*, 2017).

Owing to the diversity of leaf form—and the range of applications for data on leaf morphology—regular methodological experimentation is required so that researchers have an up-to-date toolkit with which to quantify this key plant trait. In this paper, we provide such experimentation through a quantitative morphological study of the leaves of *Ginkgo biloba* L., an extant gymnosperm that is noted for the diversity of leaf shapes that are produced by individual specimens (e.g. Leigh *et al.*, 2011). *Ginkgo* has a long evolutionary history and extinct relatives of this plant were important elements of Earth's vegetation during the Mesozoic Era (~250–65 million years ago). Fossil leaves of plants that are evolutionary ancestors of living *Ginkgo* are commonly found in sedimentary rocks, and have been widely used to reconstruct Earth's ancient atmospheres and environments using their stomatal indices and carbon isotopic composition (see Sun *et al.*, 2003; McElwain & Steinthorsdottir 2017). Our study includes a small number (24) of such fossil *Gingko* leaves.

We do not initially focus on any specific morphological features such as leaf length or the nature of the leaf margin. Instead, we take an exploratory approach to the morphology of *Ginkgo* leaves, using geometric and topological methods to reveal the features that explain the observed variation in leaf shape. Our specific aims are as follows: (1) to develop a geometric method and a topological method for quantifying leaf shape; (2) to apply these methods to the

leaves of living *Ginkgo* in order to reveal which features explain the observed variation in the shape of sampled leaves; (3) to compare the results produced by the two methods in order to explore the degree to which they reveal different aspects of morphological variation; and (4) to apply our methods to fossil leaves of ancient evolutionary relatives of living *Ginkgo* in order to confront a degree of morphological variation not present in our sample of living *Ginkgo*, and to demonstrate how they could be used to study the evolution of leaf shape through geological time.

A Dataset of Modern and Fossil Leaves

Mature and fully expanded leaves were harvested from a reproductively immature *Ginkgo biloba* tree growing in partial shade as a specimen on the campus of The Open University, UK. The specimen was ascended using a ladder and seven branches growing towards the West at approximately halfway up the specimen were removed from the trunk using a saw. Every leaf growing on each branch was plucked from the base of the petiole and dried in a plant press. A total of 468 leaves from a mixture of short-shoots and long-shoots were collected from the specimen. Each of these leaves was photographed next to a scale bar using a digital camera positioned 20cm above a light box. Twenty-two fossil leaves produced by evolutionary relatives of living *Ginkgo biloba* were extracted from the collections of the Natural History Museum in London, and two fossil leaves were extracted from the geology collections of the School of Environment, Earth and Ecosystem Sciences, The Open University (Table 1). Each fossil leaf was photographed next to a scale bar using a digital camera and the outline of each fossil was traced using Adobe Illustrator to create a digital outline of each leaf. The petioles of fossil leaves are frequently broken, distorted or completely absent as a result of the fossilization process. A central goal of our manuscript is to compare living and fossil *Ginkgo* leaves and in order to facilitate this, we have excluded the petiole from our analyses. Our analyses are therefore focussed on the shape of *Ginkgo* leaf blades. Our dataset of modern and fossil *Ginkgo* leaf images is available in the Supplementary Information.

A Geometric Approach to Quantifying the Shape of Leaves

Methods

Building on previous work using elastic curves to quantify leaf shape (Laga *et el.* 2012, 2014), we represented each *Ginkgo* leaf blade by its boundary curve, with values mapped in the plane (two dimensional Euclidean space) (Fig. 1). When considering these representations of *Ginkgo* leaves we factored out the actions of rotation and translation and reparameterization. For example, two identical leaves could each be represented by their boundary curves, but each curve could be considered distinct from one another if they differed only by rotation (a curve could be presented at 90 degrees on top of the other for instance), but our analysis factors out such actions. It is possible to also factor out the action of scaling and we do this in an analysis of leaf shape versus leaf area.

To quantitatively model morphological variation in our sample of *Ginkgo* leaves, we introduce a similarity measure for shapes that serves as the basis of statistical analysis. This is an intricate process for two main reasons: (1) the infinite dimensionality of the ensemble of all shapes; and (2) the non-linearity of shape space. To overcome this difficulty, we appeal to the concepts of Riemannian geometry, and use a Riemannian metric that quantifies the difficulty of morphing one boundary curve onto another by measuring the geodesic distance between the curves, accounting for rotations, translations and reparameterizations. This enables us to quantify shape similarity as the minimal deformation cost to reshape a curve, in this case a *Ginkgo* leaf contour. Despite the nonlinear nature of shape space, this framework allows us to calculate mean shapes and locally linearize shape data about the mean, which, in turn, lets us employ standard statistical methods on linearized data to analyse the shape variation present in our sample of *Ginkgo* leaves.

The Riemannian metric we employ is grounded on principles of linear elasticity and is formally defined on the ensemble of parametric curves, but its invariance properties ensure that it descends to a shape metric. A precise definition of the metric and a discussion of its main properties may be found in Bauer *et al.* (2017, 2019) (see also Klassen *et al*. (2004) for related shape metrics). In practice, the comparison of *Ginkgo* leaf boundary curves is a shape-matching problem, and to solve we discretized the boundary curve of each leaf using a finite dimensional representation. This reduces the problem of

comparing leaf boundary curves to a finite-dimensional optimization problem that can be solved with standard methods of numerical optimization. We use principal component analysis (PCA) to uncover the principal modes of shape variation in *Ginkgo* leaves.

The essential steps in this approach are: (1) image processing to isolate each leaf from the image background and remove the petiole; (2) find the boundary curve of each leaf blade; (3) discretize boundary curve of each leaf blade using a finite dimensional representation; (4) for each leaf blade, calculate an elastic metric that quantifies the difficulty of morphing one leaf boundary curve onto another; (5) compare leaves and visualize the dominant modes of shape variation among leaves using PCA. The code underlying our geometric approach is fully open source available at https://github.com/h2metrics/h2metrics. The provided package contains detailed documentation and user-friendly working examples.

Results

We calculated the Karcher mean of our sample of modern *Ginkgo* leaves (Fig. 1) and then locally linearized the data about the mean in order to uncover the principal modes of leaf shape variation. This was accomplished by solving a shape-matching problem between the mean and each leaf in the dataset. Principal component analysis on the linearized data indicated that approximately 30 components are needed to explain 80% of the shape variation in our sample of *Ginkgo* leaves (Fig. 2a), and we graphically display the principal modes of leaf shape variation using geodesic PCA plots (Fig. 2b–d). The first mode is predominantly leaf size (first principal component, Fig. 2b), the second mode relates to the nature of the leaf margin (second principal component, Fig. 2c), and the third and fourth modes are the depth of the furrow that separates the two lobes of the typical *Ginkgo* leaf, together with the angle of the two lobes at the base of the leaf that is also related to leaf width (third principal component, Fig. 2d). Some leaves, for example, have a very deep furrow whereas others have no furrow at all. Similarly, some leaves have lobes that are quite pointed and curve backwards towards the leaf base, whereas others have lobes that do not curve backwards.

Examples of variability in terms of the morphological features identified by our geodesic plots (Fig. 2b–d) can be seen in a PCA ordination of our dataset of *Ginkgo* leaves (Fig. 3a). Leaves towards the left are relatively small and leaves towards the right are relatively large (Fig. 3a). Leaves to the bottom are typically more dissected and have a relatively deep furrow, whereas leaves to the top are typically less dissected and have a relatively shallow furrow (Fig. 3a). This plot also highlights that the morphological space occupied by our sample of *Ginkgo* leaves, as delineated by our geometric approach, is organized as a continuous distribution of datapoints without separate clusters. Most data points are concentrated towards the center of the ordination, and the distribution of data points becomes sparser with increasing distance from the center (Fig. 3a).

A Topological Approach to Quantifying the Shape of Leaves

Methods

We employed the topological data analysis technique persistent homology (PH) (Edelsbrunner & Harer 2010; Otter *et al*. 2017; Li *et al*. 2018a,b) and represented each *Ginkgo* leaf in our dataset with a persistence barcode. To construct this barcode, for each point on the contour of a leaf (its boundary curve), we calculated the distance to the point P where the leaf blade meets the petiole (Fig. 4a). Distance was measured in pixels and in our source images 152 pixels = 1 cm. All images were downscaled by 1/8 and so 19 pixels = 1 cm in our analyses. For each $r > 0$, we counted the number of connected components formed by the points on the contour whose distance to P is greater or equal to r and recorded this count as a barcode. For example, for $r = 8.6$, there are 4 connected components (these are the uninterrupted segments of the leaf blade contour, Fig. 4a), so there are $b = 4$ bars over that value of r (Fig. 4b). Similarly, for $r = 7.0$, 5.4, 3.8, (Fig. 4a) the corresponding number of bars is b = 3, 2, 1 (Fig. 4b). The barcode summarizes the count as we gradually lower the threshold r, with bars disappearing as connected components coalesce and bars appearing as new components emerge. The coalescence of two connected components follows the elder rule: the first-born bar survives while the younger bar dies. Through this construct, we mapped the dataset of leaves to a dataset of barcodes, with each leaf described by a barcode. In order to facilitate statistical analysis, we

vectorized each barcode by listing the length of the bars in decreasing order. Since different leaves may produce barcodes with different number of bars, we padded the tails of the vectors with zeros to make all vectors the same length. In our analysis of modern leaves, statistical analyses were performed on these padded vectors. In our analysis of modern and fossil *Ginkgo* leaves combined, statistical analyses were performed on vectors that were normalized by the length of the first bar (the first component of each normalized vector was therefore 1 and discarded). The essential steps in this approach are: (1) image processing to isolate each leaf from the image background and remove the petiole; (2) find the contour curve of each leaf blade; (3) reparameterize the contour curve of each leaf blade; (4) calculate the persistent homology of each leaf blade; (5) construct the persistence barcode of each leaf blade; (6) compare leaves and visualize the dominant modes of shape variation among leaves using multi-dimensional scaling. An example of the code underlying our topological approach is available at https://github.com/Haibin9632/TDA-of-ginkgo-leaves. The provided code contains documentation and user-friendly working examples.

Results

Figure 5 shows the results of PCA applied to the vectorized barcode data. The first PC explains approximately 75% of the total variance and inspection of the PC loadings indicates that it is dominated by leaf length, followed by furrow depth. The second PC explains about 22% of the total variance mainly as variation in the depth of the furrow, followed by (negative) variation in leaf length. This ordination indicates that the morphological space occupied by our sample of *Ginkgo* leaves, as delineated by our topological approach, is organized as a continuous distribution of datapoints without separate clusters, although the majority of leaves lie in the quadrant of PC1 scores −20 to 20 and PC2 scores 0 to −20, and the leaves with PC1 scores < 0 and PC2 scores > 15 are perhaps separated from the other leaves in our sample (Fig. 5). To facilitate visualization of shape variation among our sample of *Ginkgo* leaves, the original leaf images corresponding to two discrete paths, nearly parallel to the first two principal PC axes, are highlighted in Fig. 5. These two paths show contrasting behaviour: PC1

captures a pattern in which larger leaves have a deeper furrow, whereas PC2 captures a pattern in which smaller leaves have a deeper furrow.

Application to Fossil *Ginkgo* Leaves

Visual inspection of fossil leaf boundary curves highlights that the diversity of leaf shapes in our collection of *Ginkgo* fossils is greater than that found in our sample of modern *Ginkgo* leaves (compare Fig. 1 and Fig. 6a, see also the Supplementary Information). In particular, several fossil leaves are characterised by multiple deep furrows so that leaf blades consist of multiple lobes rather than just two as in the typical *Ginkgo biloba* leaf, while other fossils have highly dissected leaf margins. This greater diversity in fossil leaf shapes is picked up by both the geometric and the topological approaches we have described, and both indicate that there are fossil leaves situated outside the total range of morphological space occupied by modern *Ginkgo* leaves (Fig. 6b,c). Both approaches also highlight that there are some fossils leaves that are very similar to modern *Ginkgo* leaves, and there are some fossil and modern leaves that overlap in morphological space (Fig. 6b,c).

However, there are differences in the degree to which modern and fossil leaves are separated in morphological space using our two approaches. Using our geometric approach, relatively small leaves with shapes characterised by multiple lobes lie outside the morphological space occupied by modern *Ginkgo* leaves, while relatively large leaves with highly dissected margins plot within the space occupied by modern leaves (Fig. 6b). In contrast, using our topological approach, both of these types of fossil leaves plot outside the morphological space occupied by modern *Ginkgo* leaves (Fig. 6c). Our topological approach very clearly captures similarities and differences between modern and fossil leaves that are expected on the basis of their visual appearance alone (Fig. 6c), whereas using our geometric approach the distinction between modern and fossil leaves is not as clear (Fig. 6b).

Discussion

Comparison of Approaches

329 The two approaches we have described in this paper measure leaf shape in
330 different ways: our geometric approach is based on analysing boundary curves
331 with an elastic metric (Fig. 2), whereas our topological approach is based on
332 measuring the number of connected components as a leaf is partitioned into
333 different segments (Fig. 4). Despite these differences, the two approaches both
334 indicate that leaf size and the nature of the furrow separating the two lobes of a
335 typical *Ginkgo* leaf are primary features that explain the observed variation in
336 leaf shape. Both approaches also distinguish the leaves of *Ginkgo* long shoots
337 from those of short shoots. The leaves of long shoots are typically smaller and
338 can have a deep wide furrow and a dissected margin, while the leaves of short
339 shoots are typically larger and can have a less pronounced furrow (Leigh *et al.*,
340 2011). These two leaf types also have different structural and hydraulic
341 properties, probably related to greater hydraulic limitation of long-shoot leaves
342 during leaf expansion (Leigh *et al.*, 2011). In the PCA summary of our geometric
343 approach, the long shoot leaves are situated to the top left of the plot with low
344 PC1 scores and high PC2 scores, and form a sparsely occupied region of
345 morphological space (Fig. 3). In the PCA summary of our topological approach,
346 the long shoot leaves are situated in the top left of the plot with low PC1 scores
347 and high PC2 scores, and form a sparsely occupied region of *Ginkgo* leaf
348 morphospace (Fig. 5).
349 There are also certain differences in the morphological features
350 pinpointed by each approach. For example, our geometric approach suggests
351 that the angle of the two lobes at the base of the leaf (also related to leaf width) is
352 an important mode of morphological variation in the population of leaves we
353 have studied (Fig. 2c), but this aspect of leaf morphology is not clearly picked up
354 by our topological approach (Fig. 5). Additionally, our topological approach is
355 able to quantify the nature of the indentations in the leaf margin more clearly
356 than our geometric approach. This is because our topological features, by design,
357 precisely measure the depth of indentations—from large furrows to minor
358 crenulations—in the leaf margin. The vectors we used in our topological analysis
359 of modern and fossil *Ginkgo* leaves were normalized by the length of the first bar,
360 and each vector therefore encodes the depths of the various indentations in the
361 leaf margin relative to absolute leaf size ordered from deep to shallow. This is

highlighted in the horizontal transect in Figure 6d: to the left are modern and fossil *Ginkgo* leaves that lack indentations, whereas to the right are leaves with increasingly complex indentations, but the size of each leaf in each highlighted group varies considerably. In the language of descriptive botany, the MDS axes highlight types of leaf dissection, with axis one representing a gradient from no dissection (low axis one scores) to many relatively deep indentations (high axis one score) (Fig. 6d), and axis two representing a gradient from few relatively deep indentations (low axis two scores) to many relatively shallow indentations (high axis two scores) (Fig. 6c). This morphological feature may only be recorded in the higher orders of variation in our geometric approach (fourth and fifth principal components for our modern *Ginkgo* leaves, see Fig. 2e,f). The two approaches we have described are therefore complementary, identifying similar primary patterns of variation, but also revealing some different aspects of morphological variation.

From the perspective of PH applied to the problem of quantifying leaf shape, previous approaches have been based on measurements of the Euler characteristic curve (Li *et al*., 2018a,b). Our approach is different in that we have constructed a persistence barcode from a count of connected components formed by points on a contour at incremental distances from the base of a leaf blade (Fig. 4), and this demonstrates an alternative means by which PH can quantify leaf shape. Oftentimes, a challenge in the use of PH is the interpretation of a persistence barcode (e.g. Otter *et al.*, 2017), but for the barcodes we have generated here, the length of the longest bar represents the largest distance to *P* (Fig. 4) and is therefore a quantifier of leaf size, while the next longest bar relates to the depth of the furrow in a *Ginkgo* leaf that displays this trait, and other smaller bars relate to the depth of smaller indentations in the leaf margin. The statistical interpretation of persistence barcodes is also challenging, and as noted by Otter *et al*. (2017, p. 3) for example, "the space of barcodes lacks geometric properties that would make it easy to define basic concepts such as mean, median, and so on". In contrast, the framework of our geometric approach allows for the calculation of mean shapes and the linearization of data around the mean, and this highlights the complementary nature of the two approaches to leaf shape we have described in this paper.

Leaf Shape Versus Leaf Area

Leaf area is trait that is intimately linked to photosynthetic capacity (Yu *et al.* 2020). In the modern world leaf area is a useful proxy for specific leaf area (the ratio of leaf area to leaf dry mass) (Wright *et al*. 2004; Yu *et* al. 2020; Shi *et al*. 2020), while during the early phases of land plant evolution leaves rapidly attained large size in a 25-fold enlargement of leaf blades during the Devonian–Carboniferous radiation (Osborne *et al.* 2004). Recently, it has been suggested that leaf shape influences or is at least correlated with leaf area indices (Lin *et al.* 2020), and we have investigated this suggestion by examining the relationship between leaf shape and leaf area in our sample of modern *Ginkgo* leaves.

To do this we first measured the area of each leaf blade using line integrals and then partitioned the leaves into four groups based on their areas (area ≤ 8, 8 < area ≤ 16, 16 < area ≤ 16, area ≥ 24; area in cm^2). We then displayed how leaf area varies across morphological space by colour-coding each of these four groups in our PCA ordinations. The colour coding highlights that for our geometric approach variation in leaf area occurs primarily along the first principal component so that leaves increase in area as their size increases (Fig. 3a). In our topological approach variation in leaf area occurs along both the first and second principal components—the boundaries between leaf area groups are orientated obliquely—indicating that leaves increase in area as their size increases and their furrows get shallower (Fig 5a).

For our geometric approach we investigated the relationship between leaf area and leaf shape further by undertaking an analysis of *Ginkgo* leaf blade shape in which we factored out the effects of scaling in the comparison of leaf boundary curves (two leaves were not considered distinct if they only differed in their area). Geodesic PCA plots show the first two principal components of our scale-invariant analysis, and show that the first principal component relates primarily to the shape of the leaf blade at its base (Fig. 2e) and the second principal component relates to the depth and width of the furrow (Fig. 2f). In a PCA ordination summarizing this analysis, leaves that have essentially the same boundary curve but belong to different area groups plot very close to each other in morphological space, and the gradient between leaf area groups is less clear

428 (Fig. 3b); both results are expected since leaf area was factored out in this
429 analysis. However, although the boundaries between area groups is less clear,
430 there remains a trend from leaves with a small area in the lower left of the
431 ordination to leaves with a large area to the right of the ordination, and there is
432 minimal overlap between leaves with an area <8cm^2 and leaves with an area
433 >24cm^2 (Fig 3b).
434 For our topological approach we investigated the relationship between
435 leaf area and leaf shape further by analysing how accurately leaf area can be
436 inferred from just the two dominant principal components of shape derived from
437 our topological representation of *Ginkgo* leaves. We estimated leaf area by
438 performing a linear regression of leaf area over the first two principal
439 components (the regression gradient points diagonally to the lower right of the
440 PCA ordination (Fig. 5a)), and then compared this estimated area to the
441 measured area of each leaf (Fig. 5b). We then quantified the discrepancy
442 between predicted and measured areas by calculating an R^2 statistic that shows
443 90% of the variation in the estimated leaf area is explained by variation in
444 measured leaf area and *Ginkgo* leaf shape, as represented by our topological (PH)
445 approach, is therefore strongly related to leaf area.
446 Taken together, our analyses of leaf shape versus leaf area suggest three
447 things. Firstly, datapoints from different area groups overlap in PCA summaries
448 of both our geometric and topological representation of *Ginkgo* leaves (Fig. 3a
449 and Fig. 5a) and this highlights that while clearly an important mode of
450 morphological variation, leaf area is not the only trait responsible for organising
451 the distribution of datapoints in *Ginkgo* leaf morphological space. This is
452 emphasized by the offset between measured leaf areas and those predicted using
453 our topological representation (Fig. 5b). Secondly, the weak leaf area trend that
454 is present in our geometric scale-free analysis (Fig. 3b), suggests that leaf area
455 may itself exert an influence on the other morphological traits such as furrow
456 depth and the nature of the leaf margin. These observations may support the
457 idea (based on work with angiosperm leaves rather than gymnosperm leaves)
458 that leaf shape may "a trait for which there are many quite varies functional
459 trade-offs" and that may be an "option that fine tunes the leaf to its conditions"
460 (Nicotra *et al*. 2011; p. 547). Finally, our observations support recent reports

that leaf shape influences or is at least correlated with leaf area indices, and provide support for the idea that leaf shape could influence leaf functional traits in the context of the leaf economic spectrum (Lin *et al.* 2020).

Looking Ahead: Image Segmentation, Fossils and Future Applications

Image segmentation—the partitioning of a digital image into multiple segments—is a key step in any study involving the computational analysis of digital imagery. In this study, the goal of image segmentation was to represent each leaf by its outline. For our sample of modern *Ginkgo* leaves we were able to achieve segmentation computationally because the leaves themselves were whole, free from damage such as indentations in the leaf margin, and the images were free from major defects such as blurring. However, for the fossil *Ginkgo* leaves we have analysed, segmentation involved tracing the outline of each fossil leaf by hand rather than delineating the leaf margin computationally. In some cases of damage to a specimen, the original undamaged margin of a leaf was extremely faint, sometimes only visible using a microscope, whereas in others the leaf margin was interrupted by a scratch or hidden by a small piece of sediment (see the Supplementary Information). In situations such as these, knowledge of the processes leading to the formation and preservation of fossil leaves was used to calibrate a restoration of the fossil outline to what was judged to be its original state. This process introduces a source of potential error that is not quantified, and future work could explore how to automate elements of this image segmentation step, perhaps using a library of fossil leaf outlines produced by manual tracing to train a classifier, or perhaps repairing defects in the leaf margin computationally using techniques from inpainting (see Bertalmio *et al*., 2000). The latter could be particularly valuable in studies of leaves where damage by insects is high such as in lowland moist tropical rainforests. Discussion of image segmentation is important because it can be a factor that limits the scope of studies that rely on the computational analysis of biological imagery. In particular, we feel that image segmentation will become a key issue if methods such as those we have described here are to be upscaled and automated to analyse large numbers of fossil leaves palaeoecologically.

The inclusion of fossil leaves in this exploratory analysis (Fig. 6) indicates that both the PH framework and geometric methods based on elastic curves have potential application to evolutionary and palaeoecological problems that require data on leaf shape in the geological past (e.g. Johnson, 1992; Leaf Architecture Working Group, 1999; Royer *et al*., 2008, 2009; Peppe *et al*. 2011; Bacon *et al.*, 2013). Shape data derived from these approaches could also be used as classifiers in machine learning work to automate the classification of leaves in studies of modern and ancient plant diversity (cf. Wilf *et al.*, 2016), and could help quantify the nature and rate of leaf shape change during development (e.g. McLellan 1993) as well as investigate how leaf shape varies as a function of a tree's aspect. Such data could also feed into the Climate Leaf Analysis Multivariate Program (CLAMP) (Wolfe 1990; Spicer 2008; Yang *et al*. 2011), which uses discrete categories to describe aspects of leaf form, and may enhance characters relating to the leaf margin (such as the regularity and closeness of leaf teeth) and the overall shape of leaves. The methods we have described could also be used to quantify other planar shapes produced by plants such as the sepals, petals, and tepals of flowers, which may enhance studies of the relationship between morphology and pollination biology (cf. Mander *et al.*, 2020). As an illustration of the potential wider applicability of our methods, the long-shoot and short-shoot leaves of our modern *Ginkgo* leaves are well separated by our topological approach with minimal overlap between these two discrete classes (Fig. 5c). Given that long-shoot leaf morphology is thought to arise from the hydraulic limitation of long-shoot leaves during development (Leigh *et* al. 2011), this highlights that our methods may be usefully applied to the problem of quantifying the relationship between morphology and the underlying physiological and developmental processes that are responsible for the generation of organic form.

Different horticultural varieties of *Ginkgo biloba*—which often have different ploidy levels ranging from haploid, to diploid and triploid to tetraploid—show considerable variety in leaf shape (Smarda *et al*., 2018). In particular, the mature leaves of haploid plants are typically relatively small; the leaves of triploid plants are relatively large with a deep central furrow, while the leaves of tetraploids are typically relatively large with an irregular margin

(Smarda *et al*., 2018). Since our sampling covered a single modern *Ginkgo* specimen, our ordinations do not summarize the total extant diversity of leaf form in *Ginkgo biloba*, and further work is necessary to quantify the relationship between leaf shape and ploidy level in living *Ginkgo biloba.* In this context, however, it is perhaps notable that the large leaves of modern *Ginkgo biloba* tetraploid cultivars are qualitatively similar to fossil specimens of the extinct species *Ginkgo digitata*: compare the leaf of a tetraploid cultivar 31—Pendula Gruga in Figure 2 of Smarda et al. (2018) with fossil_9 of our study (Table 1, Supplementary Information). In the fossil record, it is often unclear whether variation in traits such as leaf size, that are known to be highly plastic in living plants, represent the influence of environmental conditions or underlying genetic differences that form the basis of taxonomic distinction between different species. Ancient fossil species of *Ginkgo* are problematic in this respect, and it is unclear whether relatively small-leaved fossil Ginkgoaleans such as *Ginkgoites fimbriata* and relatively large-leaved fossil Ginkgoaleans such as *Ginkgo digitata* represent distinct genetically differentiated species or simply reflect a gradient of leaf morphologies (such as long-shoot and short-shoot leaves) that were produced by the same plant or species. Reports that show how leaf size and shape also varies with ploidy level in living *Ginkgo* (Smarda *et al*., 2018) add a further complicating factor to the interpretation of fossil material. With this in mind, future studies of fossil *Ginkgo* leaves using our methods could incorporate measurements of stomatal guard cell length as a measure of ploidy level, and analysing the stomatal guard cell size within fossil *Ginkgo* leaf populations of fixed size and shape classes could help to tease apart the influence of phenotypic plasticity, environmental conditions and genome evolution in the geological past (e.g. McElwain & Steinthorsdottir 2017).

Acknowledgements

We are grateful to three reviewers whose comments on a previous version of this work substantially improved the research. We are grateful to Peta Hayes for assistance with locating, accessing, and photographing fossil *Ginkgo* leaves in the collections of the Natural History Museum, London. WM acknowledges NSF grant DMS-1722995, MB was partially supported by NSF grant DMS-1953244.

Author contributions

LM and WM designed the research, LM generated the leaf dataset, HH and MB performed experiments and analysed data with input from WM. HH, MB, WM and LM wrote the manuscript. HH and MB contributed equally.

References

Bacon KL, Belcher CM, Haworth M, McElwain JC. 2013. Increased Atmospheric SO2 Detected from Changes in Leaf Physiognomy across the Triassic–Jurassic Boundary Interval of East Greenland. *PloS ONE* **8**: e60614.

Barthelemy D, Caraglio Y. 2007. Plant Architecture: A Dynamic, Multilevel and Comprehensive Approach to Plant Form, Structure and Ontogeny. *Annals of Botany* **99**: 375–407.

Bauer M, Bruveris M, Harms P, Møller-Andersen J. 2017. A numerical framework for Sobolev metrics on the space of curves. *SIAM Journal on Imaging Sciences* **10**: 47-73.

Bauer M, Bruveris M, Charon , Møller-Andersen J. 2019. A relaxed approach for curve matching with elastic metrics. *ESAIM: Control, Optimisation and Calculus of Variations* **25**: 72.

Bertalmio M, Sapiro G, Caselles V, Ballester C. 2000. Image inpainting. *SIGGRAPH '00: Proceedings of the 27th Annual Conference on Computer Graphics and Interactive Techniques* 417–424.

Bookstein FL. 1996. Biometrics, Biomathematics and the morphometric synthesis. *Bulletin of Mathematical Biology* **58**: 313–365.

Bucksch A, Atta-Boateng A, Azihou AF, Battogtokh D, Baumgartner A, Binder BM, Braybrook SA, Chang C, Coneva V et al. 2017. Morphological Plant Modeling: Unleashing Geometric and Topological Potential within the Plant Sciences. *Frontiers in Plant Science* **8**: 900.

Chitwood DH, Klein LL, O'Hanlon R, Chacko S, Greg M, Kitchen C, Miller AJ, Londo JP. 2016. Latent developmental and evolutionary shapes embedded within the grapevine leaf. *New Phytologist* **210**: 343–355.

590 **Chitwood DH, Otoni WC. 2017.** Morphometric analysis of *Passiflora* leaves: the
591 relationship between landmarks of the vasculature and elliptical Fourier
592 descriptors of the blade. *Gigascience* **6**: giw008.
593 **Johnson KR. 1992**. Leaf-fossil evidence for extensive floral extinction at the
594 Cretaceous-Tertiary boundary, North Dakota, USA. *Cretaceous Research* **13**:
595 91–117.
596 **Klassen E, Srivastava A, Mio M, Joshi SH. 2004**. Analysis of planar shapes using
597 geodesic paths on shape spaces. *IEEE transactions on pattern analysis and*
598 *machine intelligence* **26**: 372-383.
599 **Laga H, Kurtek S, Srivastava A, Miklavcic SJ. 2014**. Landmark-free statistical
600 analysis of the shape of plant leaves. *Journal of theoretical biology* **363:** 41–
601 52.
602 **Laga H, Kurtek S, Srivastava A, Golzarian M, Miklavcic SJ. 2012.** A
603 Riemannian elastic metric for shape-based plant leaf classification. *2012*
604 *International Conference on Digital Image Computing Techniques and*
605 *Applications (DICTA), IEEE,* 1–7.
606 **Leaf Architecture Working Group. 1999**. Manual of Leaf Architecture -
607 morphological description and categorization of dicotyledonous and net-
608 veined monocotyledonous angiosperms. 65p.
609 **Leigh A, Zwieniecki MA, Rockwell FE, Boyce CK, Nicotra AB, Holbrook NM.**
610 **2011**. Structural and physiological correlates of heterophylly in *Ginkgo*
611 *biloba* L. *New Phytologist* **189**: 459–470.
612 **Leigh EG. Jr. 1999**. *Tropical Forest Ecology*. Oxford University Press, New York.
613 **Li M, Duncan K, Topp CN, Chitwood DH. 2017**. Persistent homology and the
614 branching topologies of plants. *American Journal of Botany* **104**: 349–353.
615 **Li M, Frank MH, Coneva V, Mio W, Chitwood DH, Topp CN. 2018a**. The
616 persistent homology mathematical framework provides enhanced
617 genotype-to-phenotype associations for plant morphology. *Plant Physiology*
618 **177**: 1382–1395.
619 **Li M, An H, Angelovici R, Bagaza C, Batushansky A, Clark L, Coneva V,**
620 **Donoghue M, Edwards E et al. 2018b**. Topological data analysis as a
621 morphometric method: using persistent homology to demarcate a leaf
622 morphospace. *Frontiers in Plant Science* **9**: 553.

Lin S, Niklas KJ, Holscher D, Hui C, Ding Y, Shi P. 2020. Leaf shape influences the scaling of leaf dry mass vs. area: a test case using bamboos. *Annals of Forest Science* **77**: 11.

McLellan, T. 1993. The roles of heterochrony and heteroblasty in the diversification of leaf shapes in *Begonia dreigei* (Begoniaceae). *American Journal of Botany* **80**: 796–804.

Mander L, Parins-Fukuchi C, Dick CW, Punyasena SW, Jaramillo C. 2020. Phylogenetic and ecological correlates of pollen morphological diversity in a Neotropical rainforest. *Biotropica* **53**: 74–85.

McElwain JC, Steinthorsdottir M. 2017. Paleoecology, ploidy, paleoatmospheric composition, and developmental biology: a review of the multiple uses of fossil stomata. *Plant Physiology* **174**: 650–664.

McLellan T. 1993. The Roles of Heterochrony and Heteroblasty in the Diversification of Leaf Shapes in Begonia dregei (Begoniaceae). *American Journal of Botany*, **80**: 796–804.

Nicotra AB, Leigh A, Boyce CK, Jones CS, Niklas KJ, Royer DL, Tsukaya H. 2011. The evolution and functional significance of leaf shape in the angiosperms. *Functional Plant Biology* **38**: 535–552.

Osborne CP, Beerling DJ, Lomax BH, Chaloner WG. 2004. Biophysical constraints on the origin of leaves inferred from the fossil record. *Proceeding of the national Academy of Sciences, USA* **101**: 10360–10362.

Otter N, Porter MA, Tillmann U, Grindrod P, Harington HA. 2017. A roadmap for the computation of persistent homology. *EPJ Data Science* **6**: 17.

Peppe DJ, Royer DL, Cariglino B, Oliver SY, Newman S, Leight E, Enikolopov G, Fernandez–Burgos M, Herrera F et al. 2011. Sensitivity of leaf size and shape to climate: global patterns and paleoclimatic applications. *New Phytologist* **190**: 724–739.

Royer DL, Wilf P, Janesko DA, Kowalski EA, Dilcher DL. 2005. Correlations of climate and plant ecology to leaf size and shape: Potential proxies for the fossil record. *American Journal of Botany* **92**: 1141–1152.

Royer D, McElwain J, Adams J. 2008. Sensitivity of leaf size and shape to climate within Acer rubrum and Quercus kelloggii. *New Phytologist* **179**: 808–817.

656 **Royer DL, Meyerson LA, Robertson KM, Adams JM. 2009**. Phenotypic
657 plasticity of leaf shape along a temperature gradient in *Acer rubrum*. *PloS*
658 *ONE* **4**: e7653.
659 **Shi P, Li YR, Hui C, Ratkowsky DA, Yu XJ, Niinemets Ü. 2020.** Does the law of
660 diminishing returns in leaf scaling apply to vines? – Evidence from 12
661 species of climbing plants. *Global Ecology and Conservation* **21**: e00830.
662 **Smarda P, Horova L, Knapek O, Dieck H, Dieck M, Razna K, Hrubik P, Orloci**
663 **L, Papp L, Vesela K, Vesely P, Bures P. 2018.** Multiple haploids, triploids,
664 and tetraploids found in modern-day "living fossil" *Ginkgo biloba*.
665 *Horticulture Research* **5**: 55.
666 **Spicer RA. 2008.** CLAMP. *In*: V. Gornitz (Ed.), *Encyclopedia of Paleoclimatology*
667 *and Ancient Environments*. Springer, Dordrecht, pp. 156–158.
668 **Sun B, Dilcher DL, Beerling DJ, Zhang C, Yan D, Kowalski E. 2003.** Variation in
669 *Ginkgo biloba* L. leaf characters across a climatic gradient in China.
670 *Proceeding of the national Academy of Sciences, USA* **100**: 7141–7146.
671 **Thompson, D'AW. 1942.** *On Growth and Form*. Second Edition, Cambridge
672 University Press, Cambridge.
673 **Webster M, Sheets HD. 2010**. A practical introduction to landmark-based
674 morphometrics. *Paleontological Society Special Papers* **16**: 163–188.
675 **Weight C, Parnham D, Waites R. 2008**. LeafAnalyser: a computational method
676 for rapid and large-scale analyses of leaf shape variation. *Plant Journal* **53**:
677 578–586.
678 **Wilf P, Zhang S, Chikkerur S, Little SA, Wing SL, Serre T. 2016**. Computer
679 vision cracks the leaf code. *Proceeding of the national Academy of Sciences,*
680 *USA* **113**: 3305–3310.
681 **Wolfe JA. 1990.** Palaeobotanical evidence for a marked temperature increase
682 following the Cretaceous/Tertiary boundary. *Nature* **343**: 153–156
683 **Wright IJ, Reich PB, Westoby M, Ackerly DD, Baruch Z, Bongers F, Cavender-**
684 **Bares J, *et al*. 2004**. The worldwide leaf economics spectrum. *Nature* **428**:
685 821–827.
686 **Yang J, Spicer RA, Spicer TEV, Li C-S. 2011.** 'CLAMP' Online: a new web-based
687 palaeoclimate tool and its application to the terrestrial Paleogene and

Neogene of North America. *Palaeobiodiversity and Palaeoenvironments* **91**: 163–183.

Yu X, Shi P, Schrader J, Niklas KJ. 2020. Nondestructive estimation of leaf area for 15 species of vines with different leaf shapes. *American Journal of Botany* **107**: 1481–1490.

Supplementary Information

A dataset of modern and fossil *Ginkgo* leaf images.

Fig. and Table captions

Fig. 1. Collection of all 468 *Ginkgo biloba* leaves in our dataset represented by their boundary curves (black lines) with the Karcher mean leaf shape superimposed (red line).

Fig. 2. Geodesic PCA plots of *Ginkgo* leaves represented in the tangent space of the mean. Variance explained by all components (a), the first principle component (b), second principle component (c) and third principle component (d). Analysis with scaling factored out, first principle component (e) and second principle component (f).

Fig. 3. PCA ordination scatterplot (PC1 on horizontal axis, PC2 on vertical axis) showing the morphological variation among 468 modern *Ginkgo* leaves that is revealed by our geometric approach to leaf shape incorporating scale (a), and with scale factored out (b). Leaf area groups based on their areas: area ≤ 8 (red); 8 < area ≤ 16 (blue); 16 < area ≤ 16 (green), area ≥ 24 (black); area in cm^2.

Fig. 4. Schematic example showing the construction of a persistence barcode that describes the shape of a *Ginkgo* leaf. Four distances from the point *P* where the leaf blade meets the petiole are shown: r = 8.6, 7.0, 5.4, 3.8 (a). At the distance r = 8.6, there are four connected components outside the dashed line (a). At the distance r = 7.0, there are three connected components, at r = 5.4 there are two (the two lobes of the typical *Ginkgo* leaf), while at r = 3.8 there is one uninterrupted segment of the leaf blade contour outside the dashed line (a). To

721 construct a barcode that represents a leaf, we do not count the number of
722 connected components at widely spaced intervals as shown in (a). Instead, we
723 perform a count for each $r > 0$, and record the number of connected components
724 as r is gradually lowered in a barcode (b).
725
726 **Fig. 5.** PCA ordination scatterplot showing the morphological variation among
727 468 modern *Ginkgo* leaves that is revealed by our topological (PH) approach to
728 leaf shape, with datapoints coloured according to four leaf area groups (a).
729 Comparison of leaf area predicted from the first two principal components and
730 measured leaf area; the vertical offset between datapoints and the solid black
731 diagonal 1:1 line of equality indicates the discrepancy between the predicted and
732 measured areas (b). PCA ordination scatterplot with long-shoot and short-shoot
733 *Ginkgo* leaves highlighted (c).
734
735 **Fig. 6.** Collection of 24 fossil *Ginkgo* leaves, each represented by their boundary
736 curves (a). PCA ordination scatterplot (PC1 on horizontal axis, PC2 on vertical
737 axis) showing morphological variation of modern *Ginkgo* leaves (black
738 datapoints) together with fossil *Ginkgo* leaves (red datapoints) based on our
739 geometric approach, the PCs together explain 64% of the variation (b). MDS
740 ordination showing morphological variation of modern *Ginkgo* leaves together
741 with fossil *Ginkgo* leaves based on our topological approach, with a vertical
742 transect of enlarged leaves highlighted in blue (c) and a vertical transect of
743 enlarged leaves highlighted in blue (d). Modern leaves displayed with black
744 datapoints and fossil leaves displayed with red datapoints (b–d).
745
746
747
748
749
750
751
752
753

754 **Table 1.** Fossil *Ginkgo* leaves housed in the collections of the Natural History
755 Museum, London, and The Open University that we have investigated in this
756 paper.
757

Specimen Name	Accession Number	Age	Country	Location	Specimen Number (This Study)
Ginkgo cranei	NHM: V.68763	Paleocene	United States	North Dakota	fossil_1
Ginkgo cranei	NHM: V.68764	Paleocene	United States	North Dakota	fossil_2
Ginkgo gardneri	NHM: V.14834	Eocene	Scotland	Isle of Mull	fossil_3
Ginkgo gardneri	NHM: V.14838	Paleocene/Eocene	Scotland	Isle of Mull	fossil_4
Ginkgo gardneri	NHM: V.18436	Eocene	Scotland	Isle of Mull	fossil_5
Ginkgo gardneri	NHM: V.24999	Eocene	Scotland	Isle of Mull	fossil_6
Ginkgo sp.	NHM: V.2477	Eocene	Scotland	Isle of Mull	fossil_7
Ginkgo digitata	NHM: V.24587	Cretaceous	Australia	Queensland	fossil_8
Ginkgo digitata	NHM: V.39211	Jurassic	England	Yorkshire	fossil_9
Ginkgo digitata	NHM: V.13503	Jurassic	England	Yorkshire	fossil_10
Ginkgo digitata	NHM: V.10316	Jurassic	England	Yorkshire	fossil_11
Ginkgo huttonii	NHM: V.60195	Jurassic	England	Yorkshire	fossil_12
Ginkgo huttonii	NHM: V.3580	Jurassic	England	Yorkshire	fossil_13
Ginkgo huttonii	NHM: V.40511	Jurassic	England	Yorkshire	fossil_14
Ginkgo huttonii	NHM: V.39210	Jurassic	England	Yorkshire	fossil_15
Ginkgo huttonii	NHM: V.978	Jurassic	England	Yorkshire	fossil_16
Ginkgo huttonii	NHM: V.979	Jurassic	England	Yorkshire	fossil_17
Ginkgo longifolius	NHM: V.39209	Jurassic	England	Yorkshire	fossil_18
Ginkgo siberica	NHM: V.58618	Jurassic	England	Yorkshire	fossil_19
Ginkgo digitata	NHM: V.3423	Jurassic	England	Gloucestershire	fossil_20
Ginkgo digitata	NHM: V.3429	Jurassic	England	Gloucestershire	fossil_21
Ginkgo siberica	NHM: V.19238	Jurassic	Russia	Irkutsk	fossil_22
Ginkgo huttonii	Open University geology collection	Jurassic	England	Yorkshire	fossil_23
Ginkgo huttonii	Open University geology collection	Jurassic	England	Yorkshire	fossil_24

758

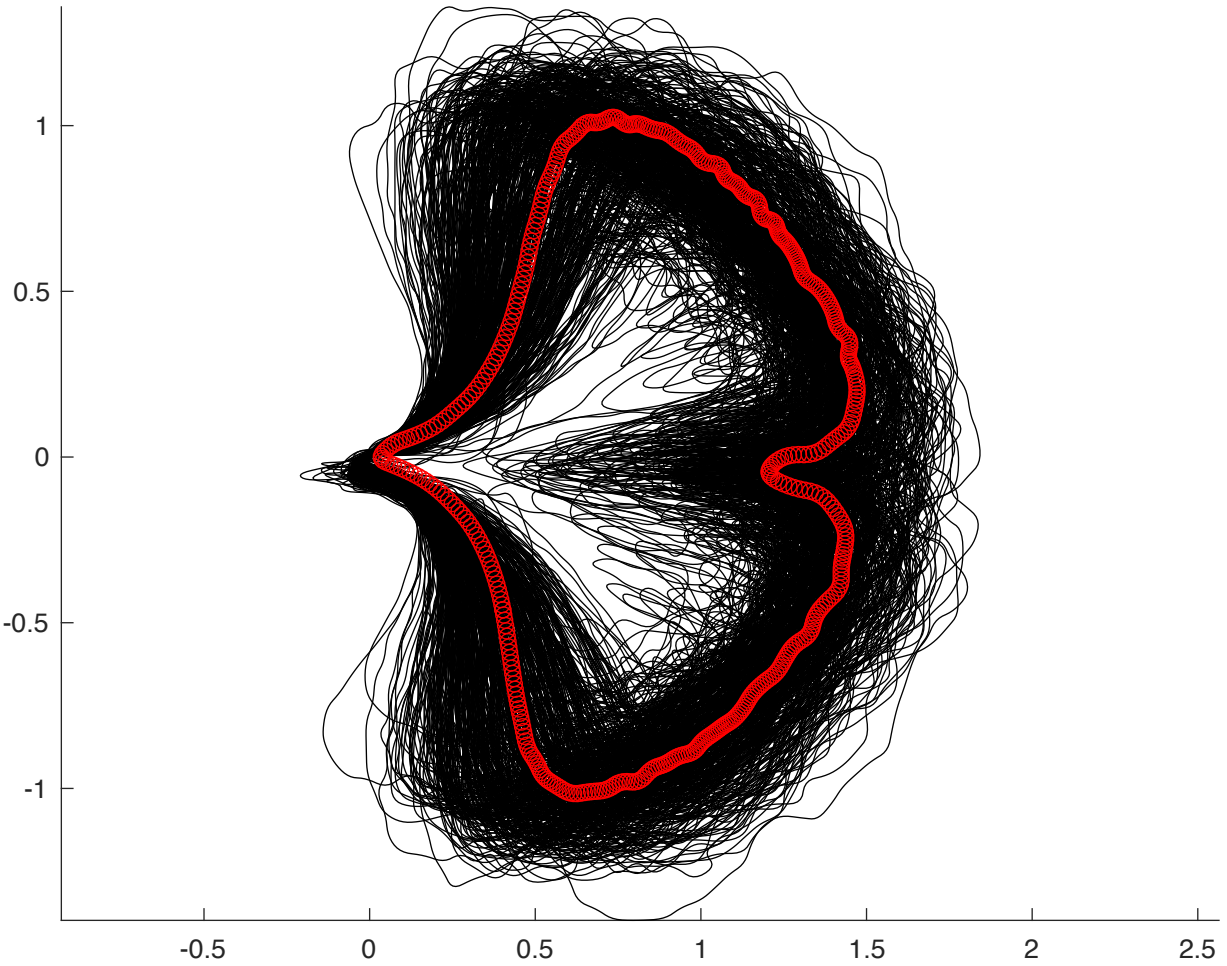
1
0.5
0
-0.5
-1
-0.5
0
0.5
1
1.5
2
2.5

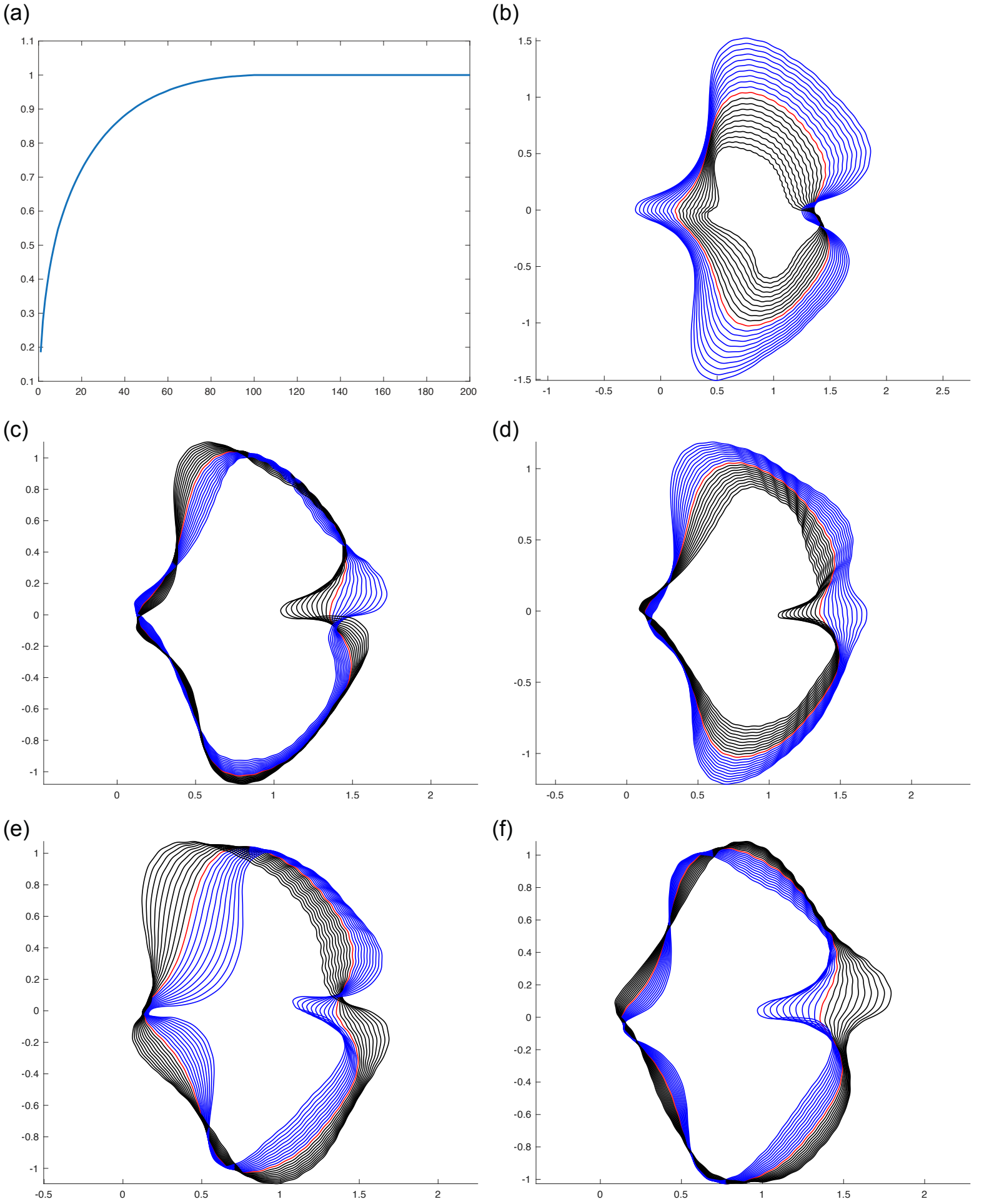
(a)
(b)
(c)
(d)
(e)
(f)

(a)

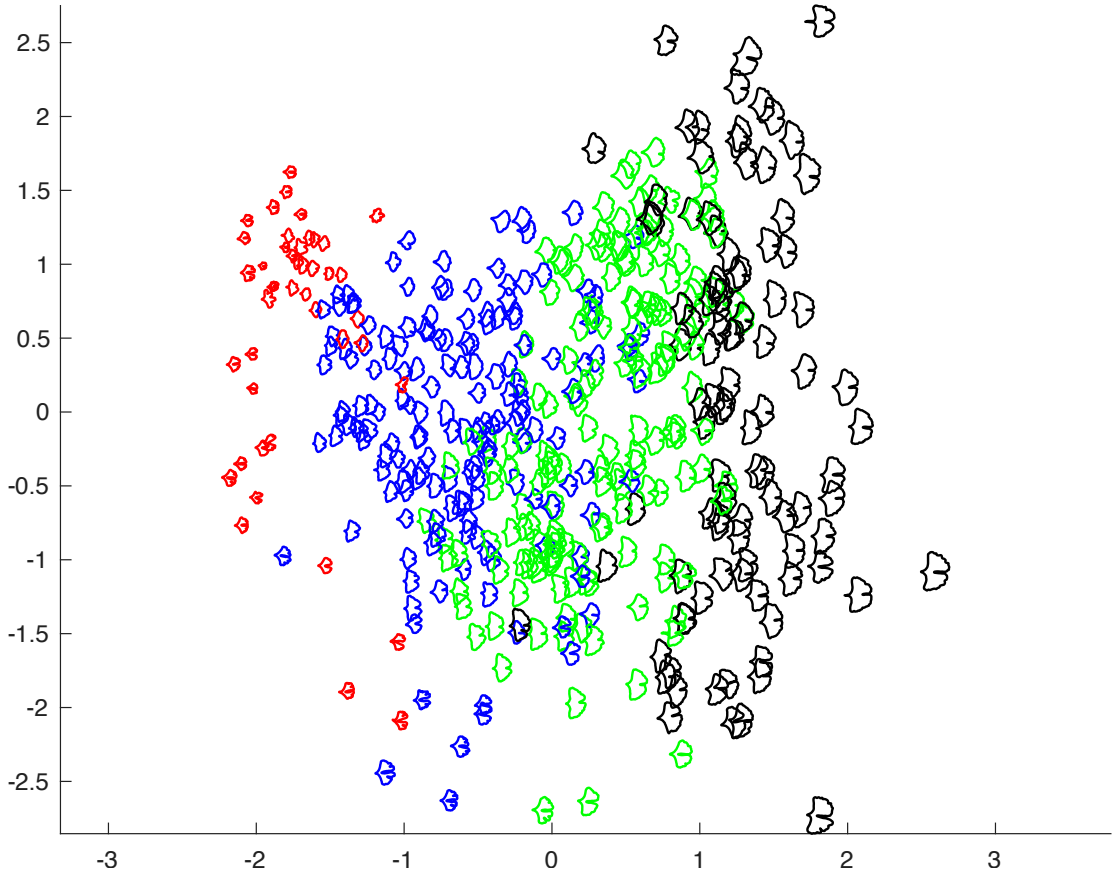

(b)

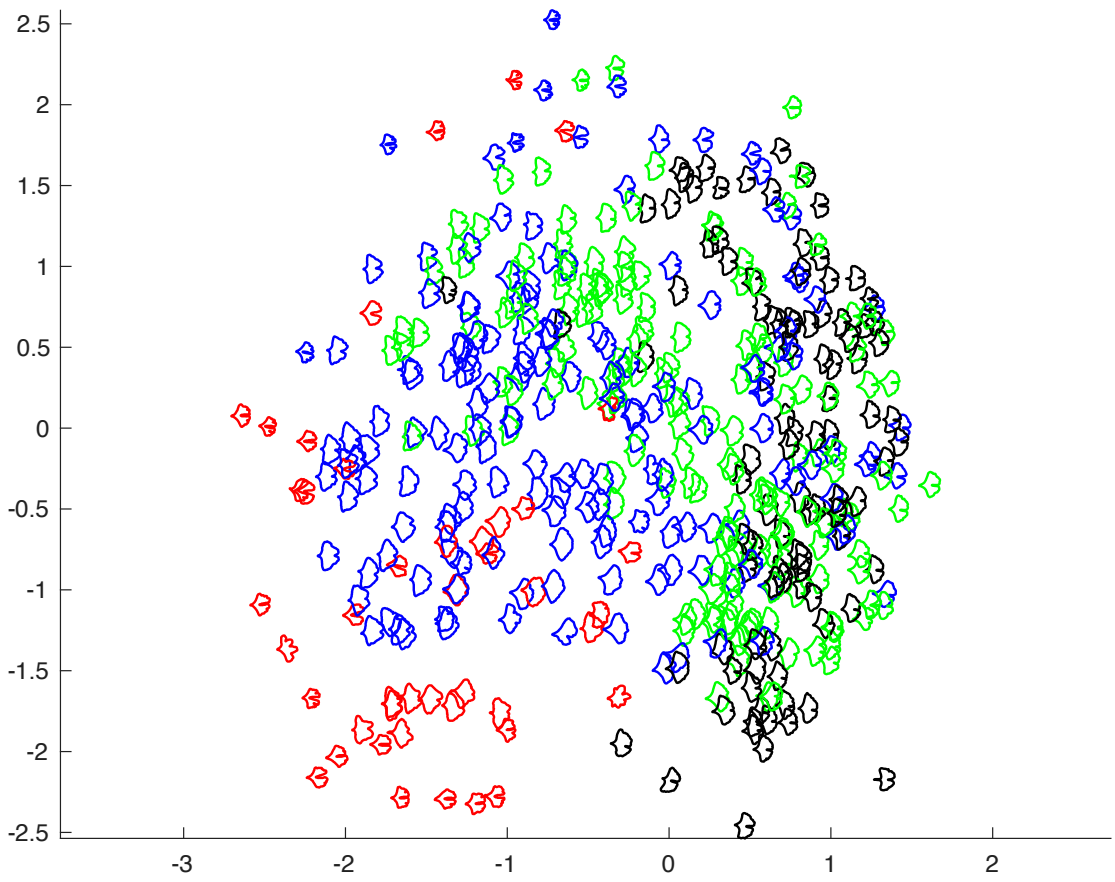

(a)

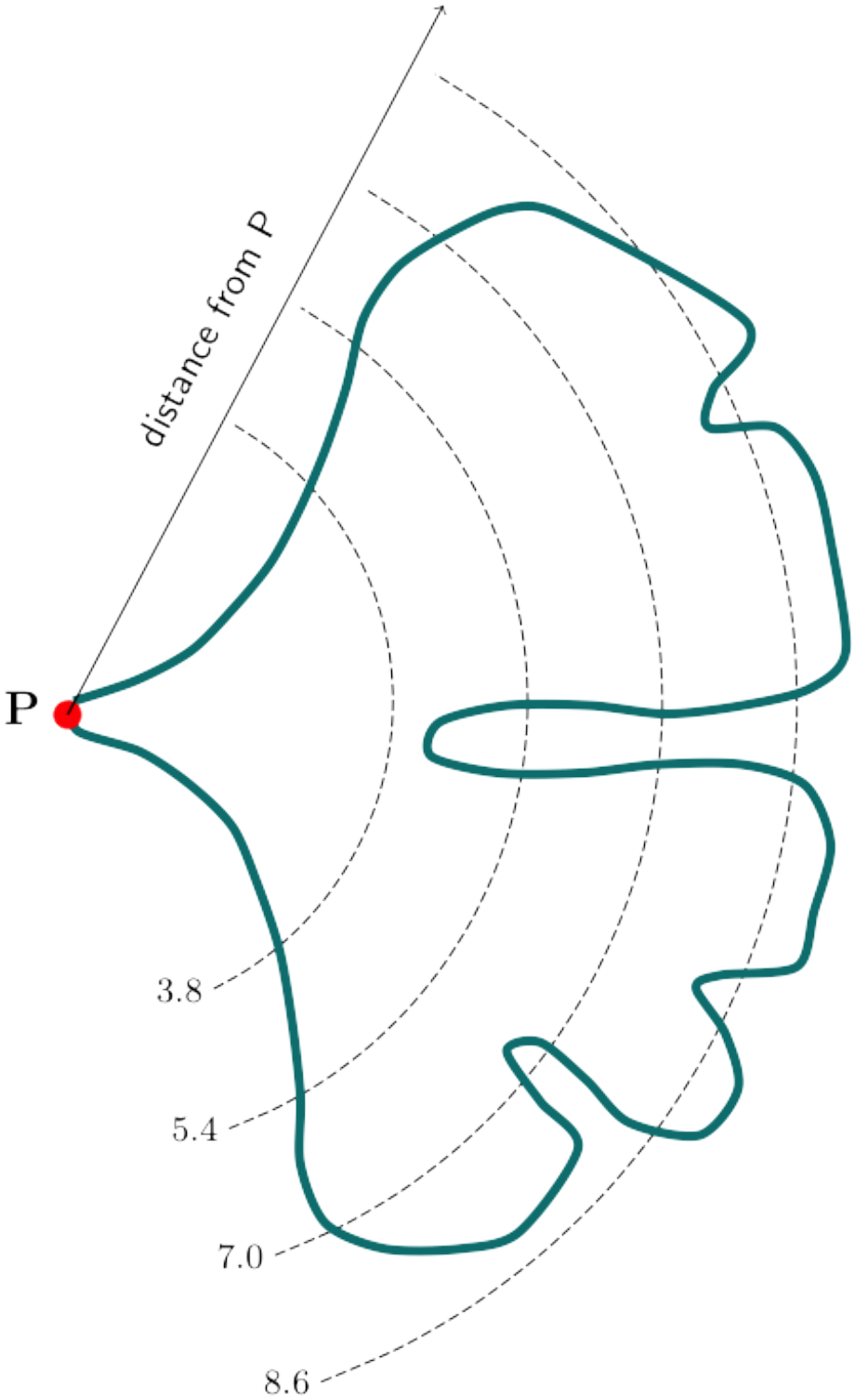

(b)

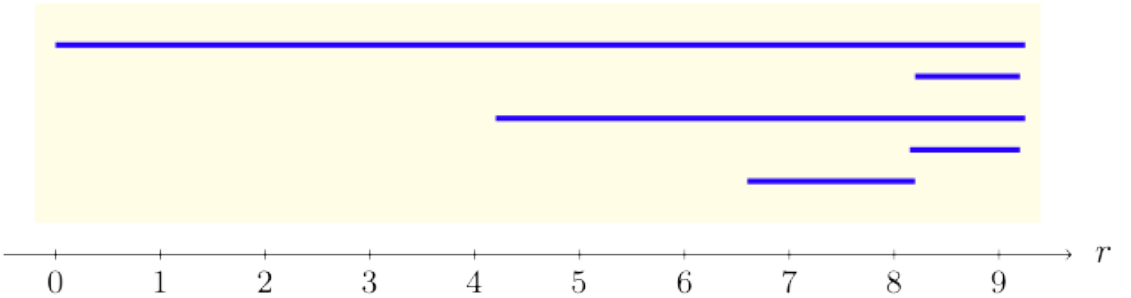

(a)

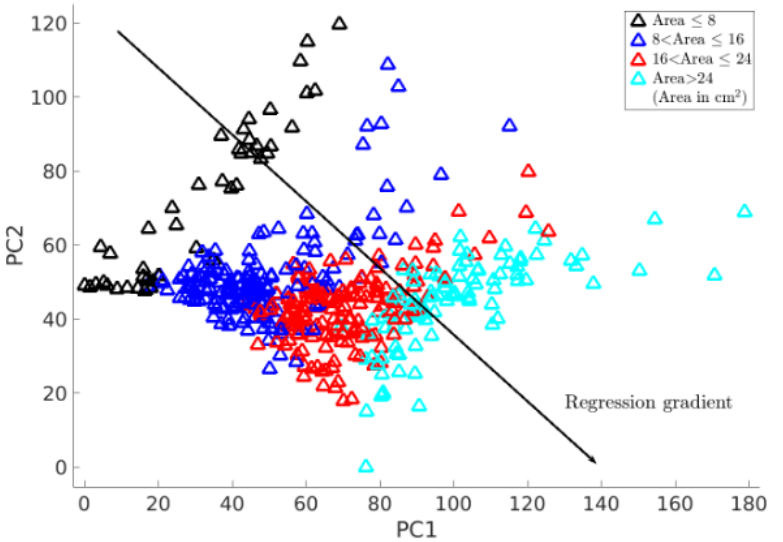
Area ≤ 8
8<Area ≤ 16
16<Area ≤ 24
Area>24
(Area in cm²)
Regression gradient
PC2
PC1

(b)

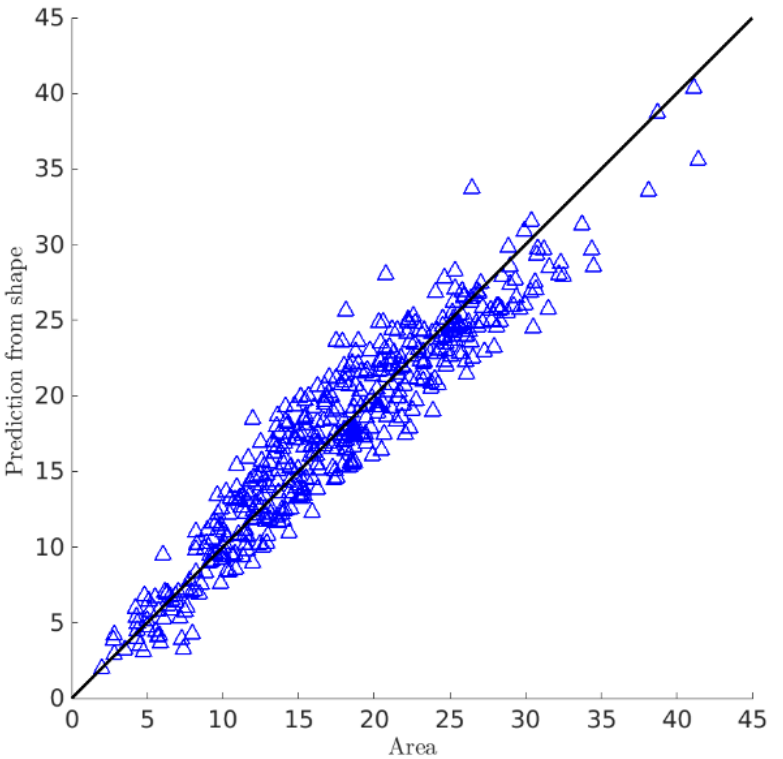
Prediction from shape
Area

(c)

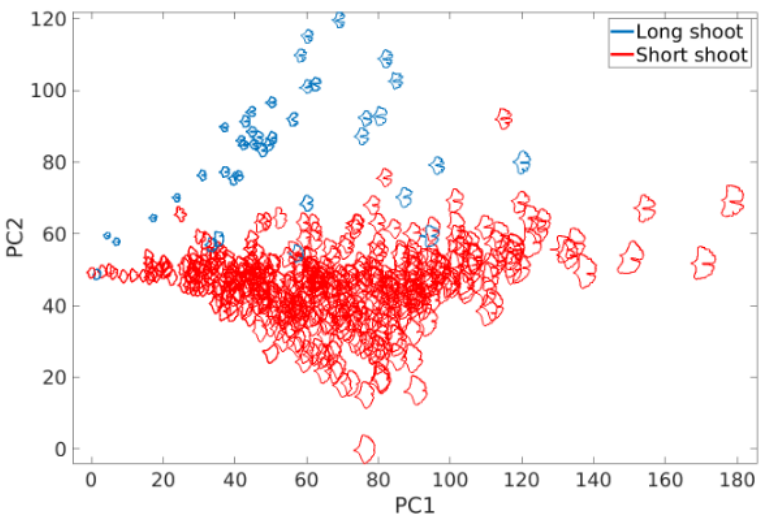
Long shoot
Short shoot
PC2
PC1

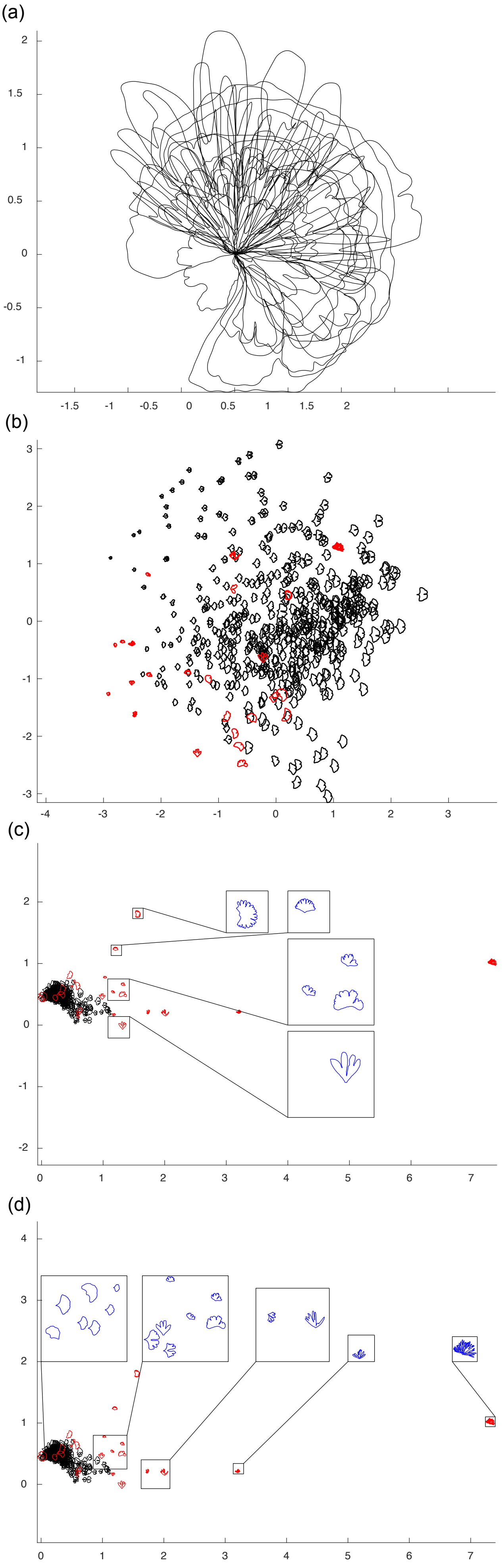
(a)
(b)
(c)
(d)